

SODIUM OLEATE AS AN EFFECTIVE CORROSION INHIBITOR FOR COPPER IN AERATED SULPHURIC ACID SOLUTIONS

Omar Abdullah Hazzazi*

Department of Chemistry, Faculty of Applied Science, Umm Al-Qura University,
P.O.Box 2897, Makkah, Saudi Arabia

(Received 21st Aug. 2006; Accepted 30th Nov. 2006)

تناولت الدراسة في هذا الجزء استخدام الملح الصوديومي لحمض الأوليك (و هو مركب له نشاط سطحي ذو شحنة سالبة) كمثبط أنيوني لتآكل النحاس في محاليل مائية من حمض الكبريت (١,٠ مولار) عند درجات حرارة مختلفة (٢٠-٧٠ درجة مئوية) وذلك باستخدام جهد الاستقطاب الديناميكي وطريقة المعاوقة الكهربائية عند جهد الدائرة المفتوحة. وتم أيضا استخدام بعض طرق التحليل (EDX) لمعرفة العناصر الموجودة على سطح الفلز في عدم وجود ووجود المثبط. وقد أوضحت النتائج أن هذا المركب يعمل على تثبيط تآكل النحاس عن طريق الامتزاز على سطح الفلز و أن معدل تثبيط تآكل النحاس يزداد بزيادة تركيز المثبط بينما يقل معدل التثبيط بارتفاع درجة الحرارة. و قد أثبتت نتائج جهد الاستقطاب الديناميكي أن هذا المثبط له القدرة على تثبيط التفاعلين المصعدي و المهبطي. و قد تم تعيين دوال الديناميكية الحرارية لعملية الامتزاز عند تراكيز مختلفة من المثبط. و قد لوحظ توافق بين نتائج طريقة جهد الاستقطاب الديناميكي و طريقة المعاوقة الكهربائية.

The inhibitive effect of sodium oleate (SO), as an anionic surfactant, on copper corrosion in aerated 1.0 M H₂SO₄ solutions in the range of temperatures (20-70°C) by means of potentiodynamic polarization and electrochemical impedance spectroscopy (EIS) techniques at the open circuit potential (OCP). The results showed that the addition of the surfactant inhibits the sulphuric acid corrosion of copper. The inhibition process was attributed to the electrostatic adsorption of the surfactant and formation of an adsorbed film on the metal surface that protects the metal against corrosive agents. Energy dispersion X-ray (EDX) observations of the electrode surface confirmed the existence of such an adsorbed film. Polarization measurements showed that the surfactant acts as a mixed-type inhibitor. The inhibition efficiency increases with increasing surfactant concentration, while it decreases with solution temperature. Maximum inhibition efficiency of the surfactant is observed around its critical micelle concentration (CMC). Temkin adsorption isotherm fits well the experimental data. Thermodynamic functions for both dissolution and adsorption processes were determined.

Key words: Copper; Sulphuric acid; Corrosion inhibition; Anionic surfactant; adsorption.

INTRODUCTION

Due to its excellent thermal conductivity, and good mechanical workability, copper is a material commonly used in heating and cooling systems. Scale and corrosion products have a negative effect on heat transfer, and they cause a decrease in the heating efficiency of the equipment, which is why periodic descaling and

cleaning in sulphuric acid (or hydrochloric acid) pickling solutions are necessary. Corrosion inhibitors effectively eliminate the undesirable destructive effect and prevent metal dissolution. Most of commercially available pickling inhibitors are toxic compounds that should be replaced with new environmentally friendly inhibitors. The corrosion of copper has been

* To whom all correspondence should be addressed; **Tel.** +96625270000 Ext. 3115;
Tel. Mob. +966553500701; E-mail address: hazzazi@hotmail.com;

studied in various solutions, and the literature on the subject has been reviewed [1-7].

Although surfactants have been widely used in the chemical and light industries and their properties has also been a subject, which has attracted many chemists' attention, only a few studies focus on the application of surfactants for corrosion prevention of metals and alloys as inhibitors [8-14]. Under appropriate conditions, enough surfactant molecules may adsorb to the solid surface, forming an organized structure, i.e., the hemimicelle [10,11], that can effectively prevent metals from corrosion in aggressive environments. In this sense, it is important to investigate the inhibition of metal corrosion by the surfactants.

This article reports the results of potentiodynamic polarization and EIS techniques complemented with some EDX observations to study the ability of sodium oleate (SO) as an anionic surfactant to inhibit the corrosion of copper in 1.0 M sulphuric acid solution under the influence of various experimental conditions including surfactant concentration, temperature and immersion time. It was also the purpose of the present work to test the experimental data obtained from the two techniques with several adsorption isotherms at different temperatures, in order to determine the thermodynamic functions for the adsorption process and gain more information about the mode of adsorption of the surfactant on the copper surface.

EXPERIMENTAL

The copper electrode was made from 99.9 % pure copper rods of 4 mm diameter. The rod specimen was embedded in an epoxy resin mould and only its cross section was allowed to contact the electrolyte solutions. The electrode was first briefly ground with no. 600 emery paper, subsequently polished with no. 2000 emery paper, and finally rinsed with alcohol and distilled water before each experiment.

The experiments were performed in a 100 cm³ volume cell at 30°C±1, using Pt wire and a SCE as auxiliary and reference electrodes, respectively. The SCE was connected via a Luggin capillary, the tip of which was very close to the surface of the working electrode to

minimize the IR drop. All potentials given in this paper are referred to this reference electrode.

The experiments were carried out in 1.0 M H₂SO₄ solutions devoid of and containing various concentrations of sodium oleate (C₁₈H₃₃O₂Na⁺) as an anionic surfactant inhibitor. The structure of the inhibitor is given below:



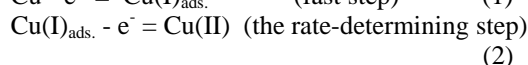
The CMC of the surfactant was determined from surface tension measurements as a function of the surfactant concentration. All solutions were freshly prepared from analytical grade chemical reagents using doubly distilled water and were used without further purification. For each run, a freshly prepared solution as well as a cleaned set of electrodes was used. Each run was carried out in aerated stagnant solutions at the required temperature (±1°C), using water thermostat. The working electrode was stabilized in 1.0 M H₂SO₄ solution for 60 min. prior to each polarization scan or impedance run. The pre-treatment served to put the electrode surface in a reproducible initial state and obtain a stable corrosion potential. The potentiodynamic current-potential curves were carried out by changing linearly the electrode potential automatically from the starting potential with respect to (SCE) towards more positive direction with the required scan rate till the end of the experiment, EIS measurements were carried out using AC signals of amplitude 5 mV peak to peak at the open circuit potential in the frequency range of 100 kHz to 10 Hz. A Potentiostat / Galvanostat (EG&G model 273), lock-in amplifier (model 5210) and M352 corrosion software and M398 impedance software from EG&G Princeton Applied Research were used for the polarization and EIS measurements, respectively. All impedance data were fit to appropriate equivalent circuits using computer program EQUIVCRT [15].

The composition and morphology of the corrosion products formed on the surface of Cu in 1.0 M H₂SO₄ solutions in the absence and presence of 10⁻³ M SO were tested at different immersion times by EDX examinations using a Traktor TN-2000 energy dispersive spectrometer. The Cu samples were finally washed thoroughly and submitted to 5 min of ultrasonic cleaning in order to remove loosely adsorbed ions.

RESULTS AND DISCUSSION

1. Polarization measurements

Figure 1 illustrates the effect of surfactant concentration on the potentiodynamic anodic and cathodic polarization curves of copper electrode in 1.0 M H₂SO₄ solution at a scan rate of 0.10 mV s⁻¹ and at 30°C. Mattsson and Bockris [16] and other research workers [17-19] studied the dissolution kinetics of copper in sulphuric acid solutions and concluded that the anodic dissolution of copper takes place in two continuous steps



where Cu(I)_{ads.} is an adsorbed species at the copper surface and does not diffuse into the bulk solution. The dissolution of copper is controlled by the diffusion of soluble Cu(II) species from the outer Helmholtz plane to the bulk solution [18-20]. Figure 1 clearly shows that the increase in SO concentration reduces both the anodic and cathodic current densities. The corrosion potential (E_{corr}) is almost unchanged

upon the addition of SO. These results indicate that the inhibitor has significant effects on retarding the reduction of dissolved oxygen and inhibiting the anodic dissolution of copper. The action of SO may be related to adsorption and formation of a barrier film on the copper surface. The formation of such a barrier film is confirmed by EDX examinations of the electrode surface (see section 6).

The influence of solution temperature on the anodic and cathodic polarization characteristics of copper electrode in 1.0 M H₂SO₄ solution containing (2.5 × 10⁻⁴ M SO) has been studied; the results are depicted in Fig. 2. It is obvious that the increase in solution temperature slightly drifts E_{corr} to the negative direction and enhances both the anodic and cathodic current densities. The electrochemical parameters (j_{corr} , E_{corr} , b_a and b_c and R_p) associated with polarization measurements for copper electrode at different SO concentrations and temperatures have been simultaneously determined (by means of a computer program M352 corrosion software from EG&G Princeton Applied Research) and listed in Tables 1 and 2, respectively.

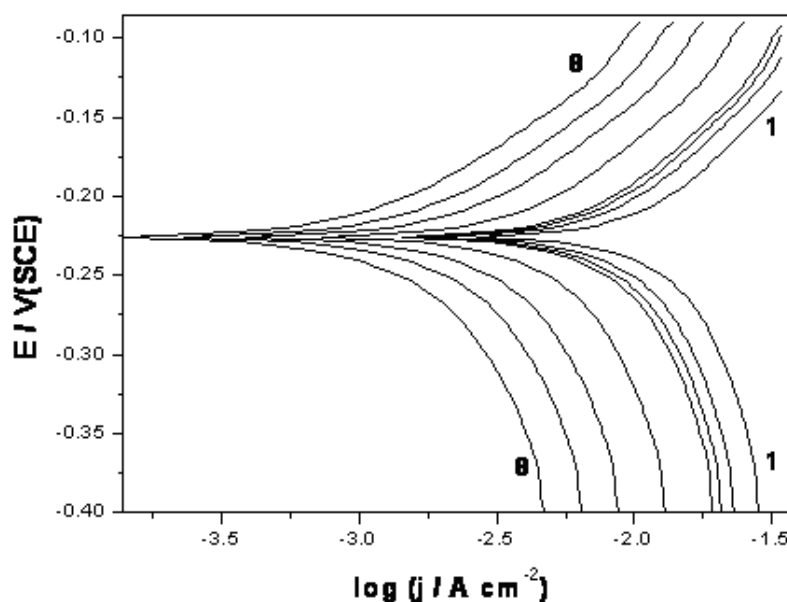


Fig. 1: Potentiodynamic anodic and cathodic polarization curves of Cu in 1.0 M H₂SO₄ solution in the absence and presence of various concentrations of SO at a scan rate of 0.10 mV s⁻¹ and at 30°C.

(1) Blank; (2) 5 × 10⁻⁵ M; (3) 8 × 10⁻⁵ M; (4) 10 × 10⁻⁵ M; (5) 25 × 10⁻⁵ M; (6) 50 × 10⁻⁵ M; (7) 75 × 10⁻⁵ M; (8) 100 × 10⁻⁵ M.

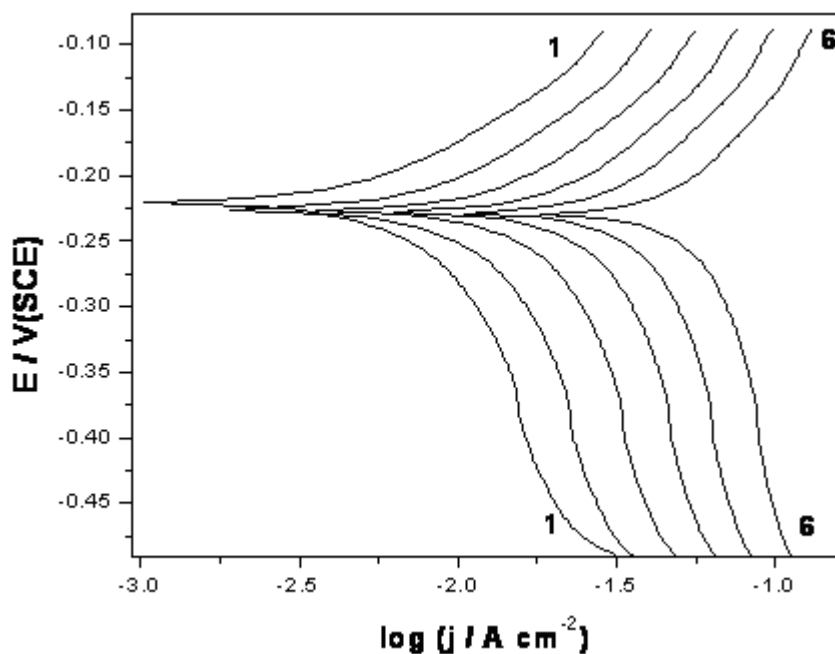


Fig. 2: Effect of temperature on the potentiodynamic anodic and cathodic polarization curves of Cu in (1.0 M H_2SO_4 + 2.5×10^{-4} M SO) solution at a scan rate of 0.10 mV s^{-1} .
(1) 20°C; (2) 30°C; (3) 40°C; (4) 50°C; (5) 60°C; (6) 70°C.

Table 1: The electrochemical parameters (j_{corr} , E_{corr} , b_c and b_a and R_p) associated with polarization measurements of Cu in 1.0 M H_2SO_4 solution in the absence and presence of different concentrations of the inhibitor at 30°C.

$C_{\text{inhib.}} \times 10^5 / \text{M}$	$j_{\text{corr}} / \text{mA cm}^{-2}$	$E_{\text{corr}} / \text{V(SCE)}$	$b_a / \text{V dec.}^{-1}$	$b_c / \text{V dec.}^{-1}$	$R_p / \text{kW cm}^2$
0.0	3.75	-0.22500	0.078	-0.128	0.992
1	3.03	-0.22495	0.077	-0.125	1.06
2	2.82	-0.22492	0.078	-0.126	1.14
5	2.32	-0.22486	0.076	-0.127	1.39
8	1.96	-0.22483	0.079	-0.128	1.65
10	1.75	-0.22478	0.077	-0.129	1.85
25	0.92	-0.22472	0.076	-0.127	3.51
50	0.49	-0.22464	0.077	-0.126	6.61
75	0.30	-0.22462	0.077	-0.129	10.62
100	0.18	-0.22457	0.078	-0.130	17.82
125	0.12	-0.22453	0.080	-0.131	26.95
150 (CMC)	0.095	-0.22448	0.078	-0.129	34.02
175	0.092	-0.22445	0.076	-0.130	35.13
200	0.09	-0.22442	0.079	-0.128	36.31

Table 2: The electrochemical parameters (j_{corr} , E_{corr} , b_c and b_a and R_p) associated with polarization measurements of Cu electrode in 1.0 M H_2SO_4 solution containing 2.5×10^{-4} M SO at different temperatures.

T / K	$j_{\text{corr}} / \text{mA cm}^{-2}$	$E_{\text{corr}} / \text{V(SCE)}$	$b_a / \text{V dec.}^{-1}$	$b_c / \text{V dec.}^{-1}$	$R_p / \text{k}\Omega$
293	0.77	-0.21910	0.077	-0.128	5.78
303	0.92	-0.22472	0.076	-0.127	3.51
313	5.13	-0.22562	0.078	-0.127	2.80
323	8.91	-0.22652	0.076	-0.128	2.37
333	14.79	-0.22743	0.078	-0.127	2.08
343	25.12	-0.22834	0.076	-0.126	1.87

It is observed from the data of Table 1 that the slopes of the anodic (b_a) and cathodic (b_c) Tafel lines remain almost unchanged upon the addition of the inhibitor. These results indicate that the adsorbed inhibitor acts by simple blocking the active sites available for both anodic and cathodic processes. In other words, the inhibitor decreases the surface area for corrosion without affecting the corrosion mechanism of copper in H_2SO_4 solutions, and only causes inactivation of a part of the surface with respect to the corrosive medium [12-14].

Since the corrosion rate is directly related to the corrosion current density (j_{corr}), the inhibition efficiencies (IE%) for copper electrode in 1.0 M H_2SO_4 solution at different SO concentrations and temperatures have been calculated following equation (3):

$$\text{IE} (\%) = 100 [1 - (j_{\text{corr}})_i / (j_{\text{corr}})_o] \quad (3)$$

where $(j_{\text{corr}})_i$ and $(j_{\text{corr}})_o$ are, respectively, the corrosion current density in the absence and presence of the inhibitor. Fig. 3 illustrates the plots of the IE (%) vs. $\log C_{\text{inhib}}$ for copper at different temperatures. The plots have S-shaped adsorption isotherms, indicating that the copper corrosion inhibition takes place through the adsorption of the surfactant on the copper surface. It is obvious that the inhibition efficiency increases with increasing SO concentration, while it decreases with temperature. The highest inhibition efficiencies are observed when SO concentration reaches values close to its critical micelle concentration (CMC). The decrease in the inhibition efficiency with increasing solution temperature could be attributed to the decrease in the strength of adsorption process at higher temperatures, suggesting that physical adsorption

may be the type of adsorption of the surfactant on the copper surface.

2. EIS measurements

Figure 4a shows the Nyquist diagram of copper electrode in 1.0 M H_2SO_4 solution at the corrosion potential. This impedance diagram is composed of a capacitive semicircle at high frequencies (HF) followed by a long Warburg diffusion tail at low frequency values. The impedance behaviour of copper in H_2SO_4 solution is somewhat similar to that of copper in HCl solution of the same concentration [21,22]. The anodic dissolution of copper in the halide-containing solutions has been proved to be diffusion limited [21,22]. The diffusion step was due to the transport of CuX_2^- to the bulk solution [22]. However, the corrosion reaction of copper in halide solutions at E_{corr} is composed of the oxidation of copper and the reduction of oxygen dissolved in the solutions [8]. The oxygen reduction is diffusion limited and usually controls the rate of the whole corrosion reaction. The diffusion of dissolved oxygen from the bulk solution to the surface of the copper electrode causes the appearance of the Warburg impedance in the corresponding impedance diagram.

If there is no oxygen dissolved in dilute H_2SO_4 solution, copper will not corrode. However, in the presence of dissolved oxygen, copper corrodes readily with the reduction of oxygen being diffusion controlled. Therefore, the appearance of the Warburg impedance spectrum for copper measured at the corrosion potential can be attributed to the oxygen diffusion from the bulk solution to the electrode surface. The HF semicircle could be attributed to the time constant of charge transfer and double layer capacitance [21,23].

Figure 4b shows the Nyquist plots recorded for copper in 1.0 M H_2SO_4 containing various concentrations of SO at 30°C. The influence of solution temperature on the impedance response of copper in (1.0 M H_2SO_4 + 2.5×10^{-4} M SO) solution has been studied; the results are depicted in Fig. 5. All impedance measurements were carried out at the respective corrosion potentials. It is clear that the shapes of the impedance plots for inhibited electrodes are not substantially different from those of uninhibited electrodes. The presence of the inhibitor increases the impedance but does not change other aspects of the behaviour. This means that the inhibitor does not alter the electrochemical reactions responsible for corrosion. It inhibits corrosion primarily through its adsorption on the metal surface.

It is essential to develop the appropriate models for the impedance, which can then be used to fit the experimental data and extract the parameters, which characterize the corrosion process. An equivalent circuit of four elements depicted in Fig. 6 was used in simulation of the impedance data. In this circuit, R_s is the solution resistance, C_{dl} the double layer capacitance, R_p

the polarization resistance, and W the Warburg impedance. One constant phase element (CPE) was substituted for the capacitive element to give a more accurate fit [8]. The measured complex plane impedance plot is similar to that calculated by the equivalent circuit models. The points in Fig. 4a represent the experimental data, while the solid curves represent the best fits.

The numerical values of the polarization resistance (R_p) and the double layer capacitance (C_{dl}) for the inhibitor were determined by analysis of the complex plane impedance plots and the equivalent circuit model by means of a computer program (M398 impedance software from EG&G Princeton Applied Research). Figure 7 represents the dependence of both R_p and C_{dl} on the logarithmic concentration of the inhibitor. It is obvious that the diameter of the capacitive loop increases, and therefore R_p values increase, with increasing SO concentration, while the C_{dl} values tend to decrease. The decrease in C_{dl} values is due to the adsorption of SO on the metal surface [24]. The reverse changes produced by increasing temperature, as shown in Fig. 5.

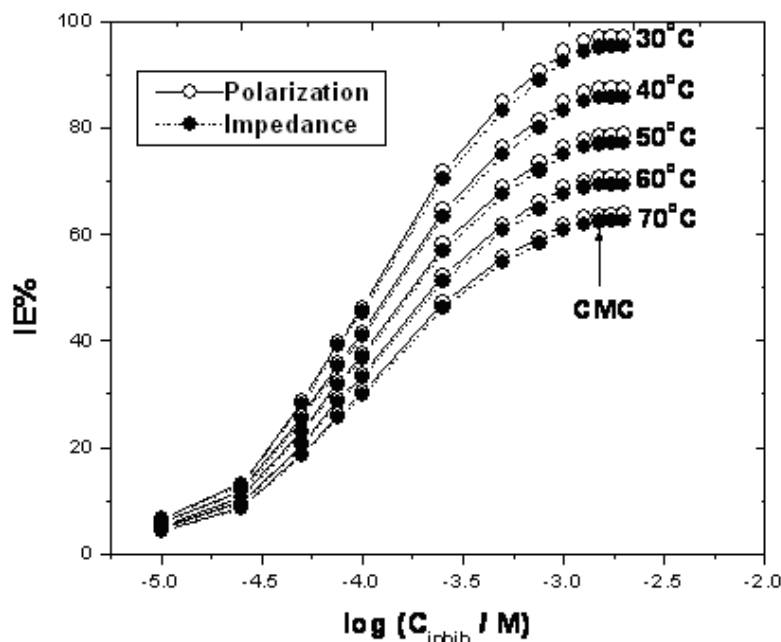


Fig. 3: The dependence of the inhibition efficiency (IE%), calculated from the polarization and impedance data, on the logarithmic concentration of the inhibitor ($\log C_{\text{inhib}}$) for Cu in 1.0 M H_2SO_4 solution at different temperatures.

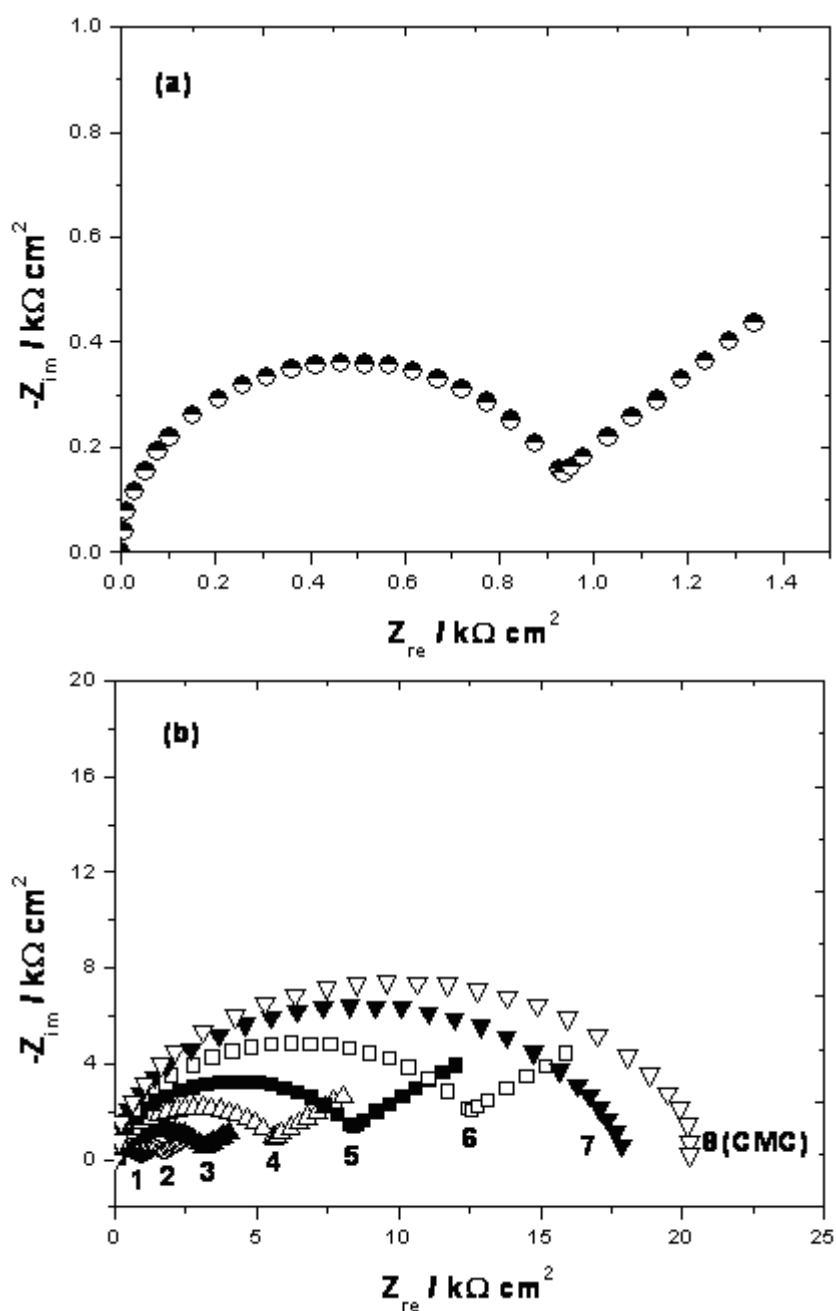


Fig. 4: (a) impedance response of Cu in 1.0 M H_2SO_4 solution at the OCP and at 30°C. (b) impedance response of Cu in 1.0 M H_2SO_4 solution containing various concentrations of SO solution at the respective corrosion potentials and at 30°C. (1) Blank; (2) 10×10^{-5} M; (3) 25×10^{-5} M; (4) 50×10^{-5} M; (5) 75×10^{-5} M; (6) 100×10^{-5} M; (7) 125×10^{-5} M; (8) 150×10^{-5} M (CMC).

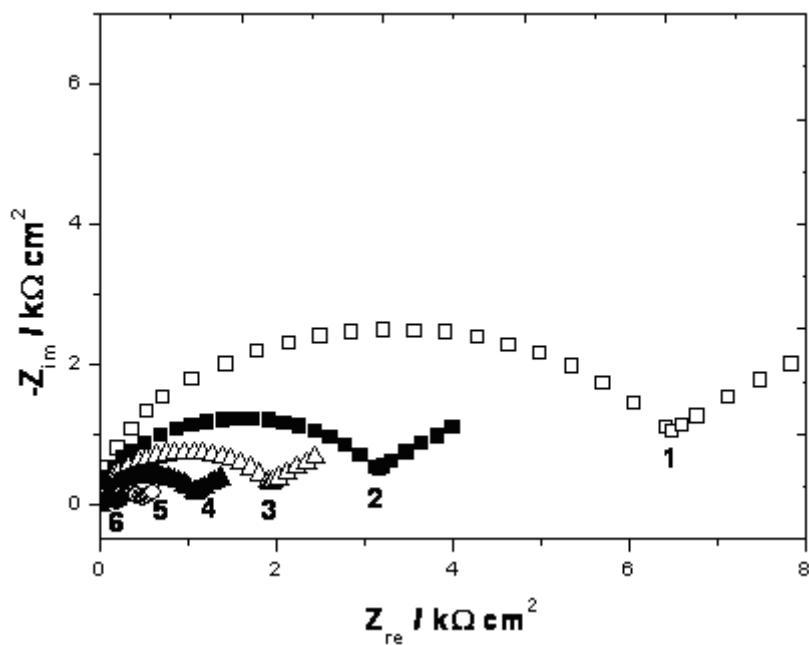


Fig. 5: The influence of solution temperature on the impedance responses of a Cu electrode in 1.0 M H_2SO_4 solution containing 2.50×10^{-4} M SO at the respective corrosion potentials. (1) 20°C; (2) 30°C; (3) 40°C; (4) 50°C; (5) 60°C; (6) 70°C.

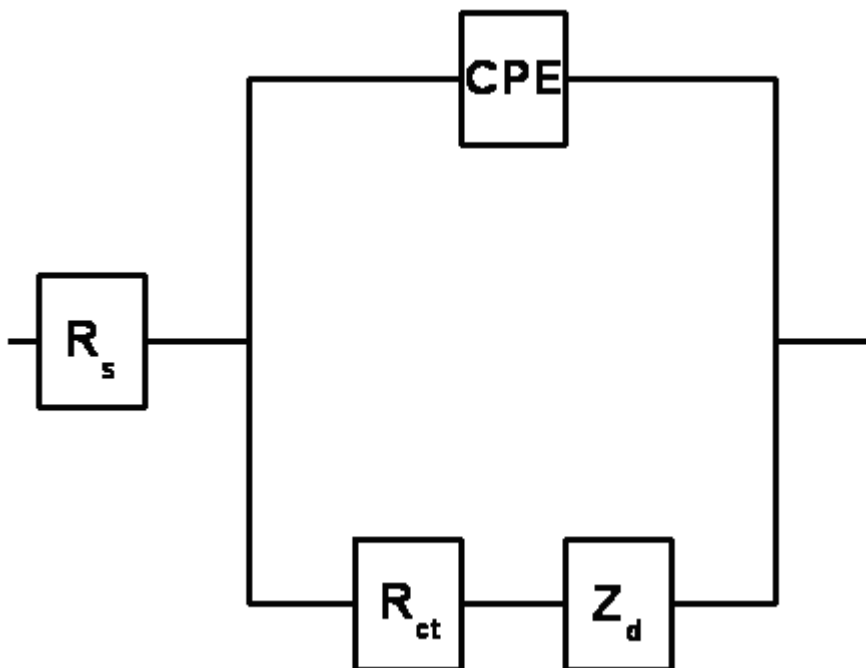


Fig. 6: The equivalent circuit used to fit the EIS data.

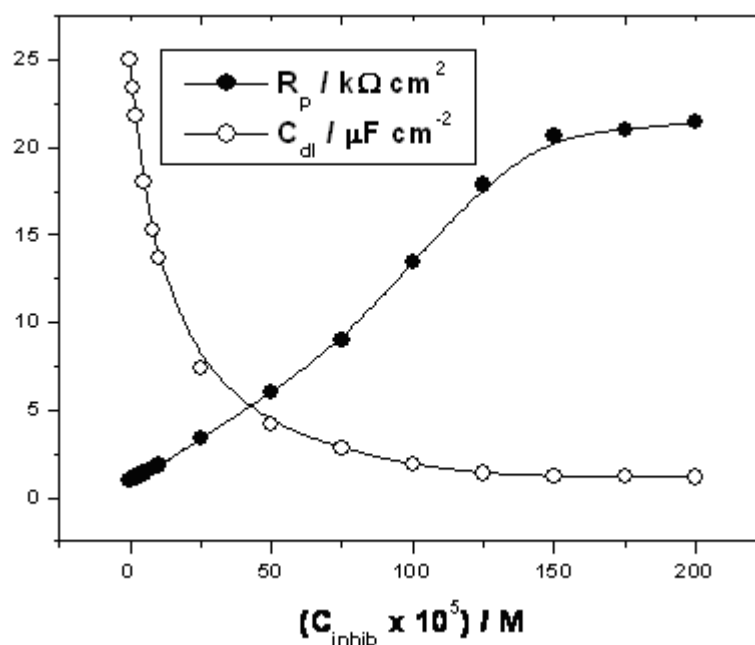


Fig. 7: The variation of both R_p and C_{dl} with SO concentration at the OCP and at 30°C.

The obtained R_p values were used to calculate the IE% of SO at different concentrations and temperatures (see Fig. 3), using equation 4.

$$\text{IE}\% = 100 \times [(R_p - R_p^0) / R_p] \quad (4)$$

where R_p^0 and R_p are the polarization resistances for uninhibited and inhibited solutions, respectively. It is apparent that the inhibition efficiency increases with increasing inhibitor concentration, and tends to attain a maximum value when the concentration reaches value close to its critical micelle concentration. Moreover, the inhibition efficiency decreases with increasing temperature, confirming the suggestion that physical adsorption is the type of adsorption of the inhibitor on the copper surface. It is worthy noting from Fig. 3 that the inhibition efficiencies obtained from impedance measurements are comparable and run parallel with those obtained from potentiodynamic polarization method.

The polarization curves in Fig. 1 have shown that SO inhibited both the cathodic and anodic reactions. The impedance spectra for copper in the SO-containing H_2SO_4 solutions at the corrosion potentials showed that the Warburg impedance

almost disappeared at higher concentrations close to CMC (see curves 7 and 8 in Fig. 4b). In addition, the impedance spectra did not display new LF capacitive (or inductive) loops in addition to the well-known HF semicircle. Thus, we can draw a conclusion that SO is a kind of mixed-type inhibitor for copper corrosion in H_2SO_4 acid solutions.

3. Effect of immersion time

Electrochemical impedance spectroscopy is a useful technique for long time tests, because they do not significantly disturb the system and it is possible to follow it overtime [25]. Immersion time experiments in the present work were carried out in (1.0 M H_2SO_4 + 2.5×10^{-4} M SO) solution for 720 min and Nyquist plots were recorded every 10 min during the first hour, and then every 60 min afterward. The results obtained (not shown here) showed that the immersion time has a great influence on the size and shape of the impedance spectra, and therefore the inhibition efficiency of SO. The capacitive loop was found to increase in size with the increase of immersion time, reaching a maximum in 50 min and remained fairly constant afterward. The Warburg impedance was

still visible during the initial 50 min and then disappeared.

More details are shown in Fig. 8, which represents the variation of both R_p and C_{dl} with the immersion time. It is obvious that the R_p values increased sharply from 3.37 to 47.53 $k\Omega\text{ cm}^2$ during the initial 50 min and remained fairly constant afterward. At the same time, the capacitance values were reduced drastically from 7.41 to 0.53 $\mu\text{F/cm}^2$ after 50 min. These results demonstrate that the formation of the inhibitor surface film, and therefore the inhibitor adsorption, on the copper surface was relatively fast and completed within 50 min.

4. Mode of adsorption of the surfactant on the copper surface

An inhibitor usually realises its inhibitive action by adsorption as a thin film onto the surface of a corroding metal or by inducing formation of a thick corrosion product. Adsorption depends mainly on the charge of the metal surface, the charge or the dipole moment of inhibitors, and the adsorption of other ionic species [10]. The potential of zero charge (pzc) plays a very

important role in the electrostatic adsorption process. It is possible to determine whether the charge of electrode surface is positive or negative from the difference between the corrosion potential and pzc of a corroding metal. According to the work of Ma et. al. [8], the pzc of copper in H_2SO_4 solutions is estimated as -140 mV (SCE), which is more negative than the corrosion potential {-96 mV(SCE)}. This means that the copper surface is positively charged at the corrosion potential. If only considering the electrostatic attraction, it is likely that the anionic surfactant will directly adsorb on the copper surface, forming a barrier on the copper surface. At the early stages of adsorption (low surface coverage), i.e., at low SO concentrations and at low immersion times, the adsorption of the hydrocarbon chain (due to the presence of "-CH=CH-" group) and the electrostatic adsorption of the oleate ions on the copper surface take place simultaneously. This model of adsorption enables the adsorbed oleate ions to cover much area, thereby inhibiting more effectively the copper corrosion.

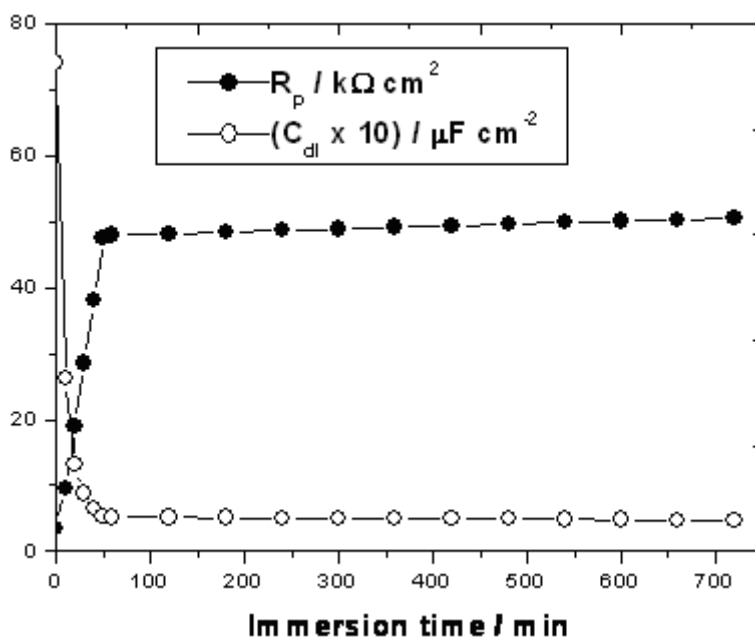


Fig. 8: The dependence of both R_p and C_{dl} on on the immersion time for cu in $\text{M H}_2\text{SO}_4$ solution containing 2.50×10^{-4} M SO solution at the OCP and at 30°C.

When the immersion time and SO concentration increased, more oleate ions will electrostatically adsorb on the copper surface. In this case, the physisorption of hydrocarbon chain may be ignored. A hemimicelle barrier composed of oleate ions will form on the whole surface due to the interaction between hydrocarbon chains via the van der Waals forces. The barrier becomes more compact and protective with adsorption of more oleate ions on the surface. In this way, the inhibition efficiency of SO increases with the increase of immersion time and concentration.

5. Adsorption isotherms

The adsorption of inhibitor molecules from aqueous solutions can be regarded as a quasi-substitution process between the organic compound in the aqueous phase $\text{Org}_{(aq)}$ and water molecules at the electrode surface, $\text{H}_2\text{O}_{(s)}$



where x , the size factor, is the number of water molecules displaced by one molecule of organic inhibitor. Adsorption isotherms are very important in determining the mechanism of organo-electro-

chemical reactions [26]. The most frequently used isotherms are Langmuir, Frumkin, Hill de Boer, Parsons, Temkin, Flory-Huggins and Dahar-Flory-Huggins and Bockris-Swinkiel [27-35]. All these isotherms are of the general form:

$$f(\theta, x) \exp(-2a\theta) = KC \quad (6)$$

where $f(\theta, x)$ is the configurational factor which depends upon the physical model and the assumptions underlying the derivation of the isotherm, θ the surface coverage degree ($\theta = \text{I.E.}/100$), C the inhibitor concentration in the bulk of solution, "a" the lateral interaction term describing the molecular interactions in the adsorption layer and the heterogeneity of the surface and is a measure for the steepness of the adsorption isotherm. K the adsorption-desorption equilibrium constant. In this study, Temkin adsorption isotherm, given by equation 7 [36], fits well with the experimental data obtained from the polarization and impedance measurements (see Fig. 9).

$$\exp(2a\theta) = KC \quad (7)$$

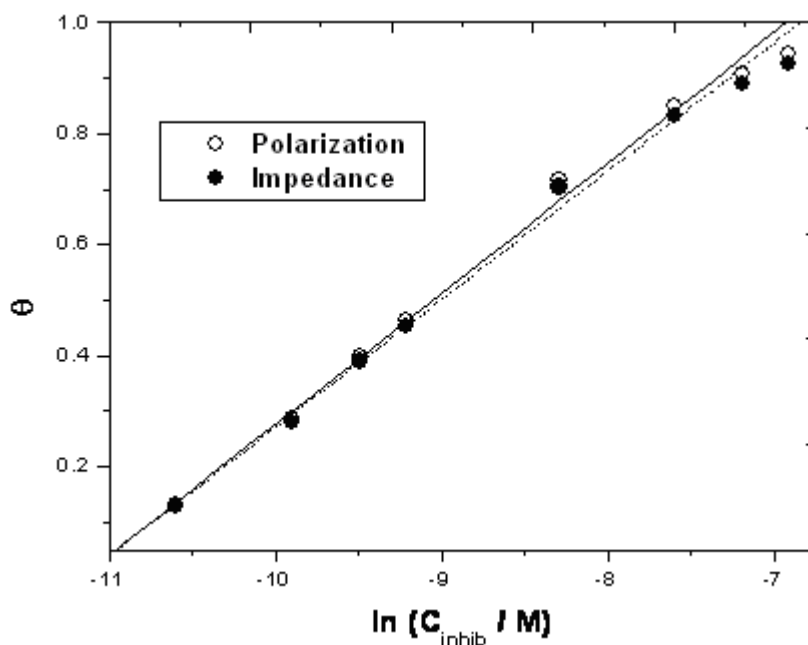


Fig. 9: Curve fitting of polarization and impedance data obtained for Cu in M H_2SO_4 solution containing 2.50×10^{-4} M SO to Temkin isotherm at 30°C .

The isotherms' parameters (K and a) recorded for copper in 1.0 M H₂SO₄ solution containing 2.5 × 10⁻⁴ M SO obtained from the two techniques at different temperatures are listed in Table 3. It is obvious that the values of K decrease with an increase in temperature. Large values of K mean better inhibition efficiency of the inhibitor, i.e., strong electrical interaction between the double layer existing at the phase boundary and the adsorbing inhibitor molecules. Small values of K, however compromise that such interactions between adsorbing inhibitor molecules and the metal surface are weaker, indicating that the inhibitor molecules are easily removable by the solvent molecules from the surface. These results confirm the suggestion that this inhibitor is physically adsorbed on the metal surface and the strength of the adsorption decreases with temperature. High and positive values of "a" would indicate the existence of relatively strong lateral forces of attraction between adsorbate molecules in the adsorption layer [37]

The free energies of adsorption calculated from equation 8 [35]:

$$K = (1/55.5) \exp(-\Delta G_{\text{ads}}^{\circ}/RT) \quad (8)$$

are shown in Table 4, where $\Delta G_{\text{ads}}^{\circ}$ is the free energy of adsorption, 55.5 the concentration of water in the solution in mol l⁻¹, R the universal gas constant, T the thermodynamic temperature. The negativity of the free energies of adsorption,

shown in Table 4, means that the adsorption process is spontaneous.

It follows from the theory of adsorption from solutions [37] that:

$$(d \ln K/dT)_{\theta} = -\Delta H_{\text{ads}}^{\circ}/RT^2 \quad (9)$$

Where $\Delta H_{\text{ads}}^{\circ}$ is the isosteric enthalpy of adsorption. The integrated version of the Vant Hoff equation:

$$\ln K = -\Delta H_{\text{ads}}^{\circ}/RT + \text{constant} \quad (10)$$

may be used to determine $\Delta H_{\text{ads}}^{\circ}$. The slopes of the lines, shown in Fig. 10, depict the linear relation between lnK and (1/T) at a given surface coverage. These slopes, multiplied by R, give the values of $\Delta H_{\text{ads}}^{\circ}$ shown in Table 4. The values of the entropy change of the inhibitor adsorption ($\Delta S_{\text{ads}}^{\circ}$), listed in Table 4, was calculated from the equation:

$$\Delta G_{\text{ads}}^{\circ} = \Delta H_{\text{ads}}^{\circ} - T \Delta S_{\text{ads}}^{\circ} \quad (11)$$

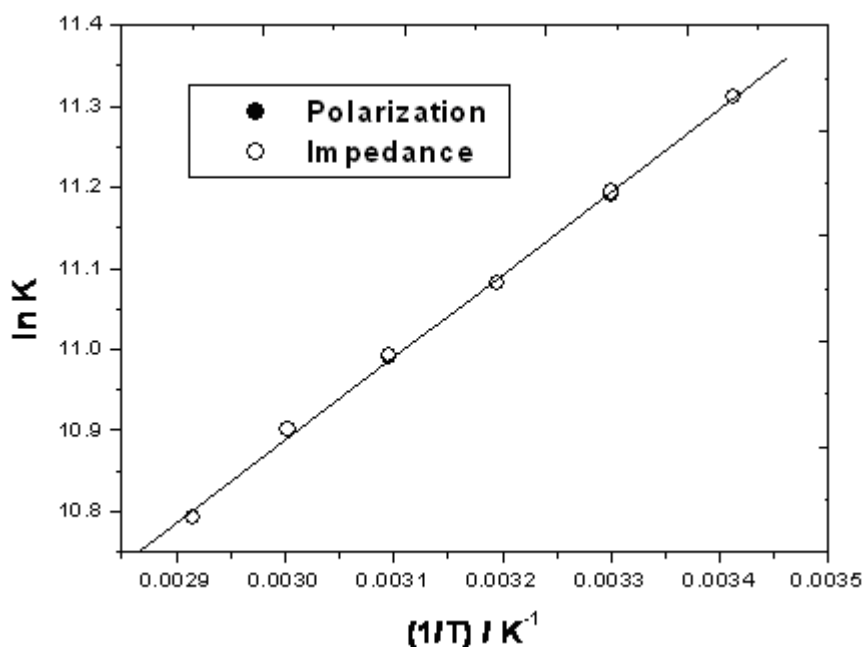
It is obvious from the data presented in Table 4 that the absolute value of the adsorption enthalpy, $|\Delta H_{\text{ads}}^{\circ}|$, increases with the increase in surface coverage due to the attractive interaction between the adsorbed molecules indicating the validity of the Temkin model [36]. The origin of the attractive forces is most probably the dipole-dipole interaction occurring between the neighbouring adsorbed molecules [38]. The negativity of the enthalpy means that heat is released from the adsorption process.

Table 3: Values of "K" and "a" for Cu in 1.0 M H₂SO₄ solution containing 2.50x10⁻⁴ M SO obtained by applying Temkin isotherm on the polarization and impedance data at different temperatures.

T / K	Temkin isotherm			
	K		.a	
	Polarization	Impedance	Polarization	Impedance
293	81782	81800	2.10	2.15
303	72511	72700	2.13	2.17
313	64976	64980	2.15	2.19
323	59384	59405	2.18	2.21
333	54270	54285	2.22	2.25
343	48615	48635	2.26	2.29

Table 4: The thermodynamic parameters of adsorption process obtained from the polarization and impedance data by applying Temkin isotherm for Cu in 1.0 M H₂SO₄ solution containing various concentrations of SO at OCP and at 30°C.

$C_{\text{inhib.}} \times 10^5 / \text{M}$	Polarization measurements			Impedance measurements		
	$\text{DH}_{\text{ads}}^{\circ} / \text{kJ mol}^{-1}$	$\text{DG}_{\text{ads}}^{\circ} / \text{kJ mol}^{-1}$	$\text{DS}_{\text{ads}}^{\circ} / \text{J mol}^{-1} \text{K}^{-1}$	$\text{DH}_{\text{ads}}^{\circ} / \text{kJ mol}^{-1}$	$\text{DG}_{\text{ads}}^{\circ} / \text{kJ mol}^{-1}$	$\text{DS}_{\text{ads}}^{\circ} / \text{J mol}^{-1} \text{K}^{-1}$
1	-4.90	-25.14	67.92	-4.84	-25.10	68.00
2	-6.45	-26.41	66.98	-6.40	-26.38	67.05
5	-7.84	-28.16	64.90	-7.78	-28.12	65.00
8	-8.75	-30.20	60.67	-8.71	-30.00	60.23
10	-9.25	-30.82	54.00	-9.18	-30.70	53.70
25	-10.45	-31.76	51.81	-10.34	-31.79	53.02
50	-23.50	-34.42	36.64	-23.25	-34.35	37.25
75	-30.74	-36.05	17.82	-30.62	-35.96	17.92
100	-36.00	-36.51	1.71	-35.92	-36.40	1.61
125	-37.00	-36.78	-0.74	-36.96	-36.65	-1.04
150 (CMC)	-37.65	-37.00	-2.18	-37.25	-36.91	-1.14
175	-38.05	-37.34	-2.38	-37.91	-37.06	-2.85
200	-38.35	-37.50	-2.68	-38.30	-37.40	-3.02

**Fig. 10: The relation between log (binding constant) and 1/T for Cu in 1.0 M H₂SO₄ solution containing 2.50 × 10⁻⁴ M SO at 30°C obtained by applying Temkin adsorption isotherm on polarization and EIS data.**

Generally, an exothermic adsorption process signifies either physi- or chemi-sorption, while endothermic process is attributable unequivocally to chemi-sorption [39]. In an exothermic process, physi-sorption is distinguished from chemi-sorption by considering the absolute value of adsorption enthalpy. Typically, the enthalpy of a physi-sorption process is lower than $41.86 \text{ kJ mol}^{-1}$, while that of a chemi-sorption process approaches 100 kJ mol^{-1} [40,41]. In the present work, the absolute values of enthalpy are relatively low approaching those typical of physi-sorption.

Table 4 clearly shows that the values of $\Delta S_{\text{ads}}^{\circ}$ decrease with increasing inhibitor concentration. The entropy changes can be explained in terms of displacement of the H_2O molecules from the surface into the hydrogen-bonded aqueous solution and adsorption of surfactant molecules at the surface from their surface-active positions in the solution phase.

6. EDX examinations of the electrode surface

EDX survey spectra were used to determine which elements were present on the copper surface before and after exposure to the inhibitor solution. Figure 11 presents spectra for copper samples exposed for 30, 60, 90, 120, 150, 180 and 210 min in 1.0 M H_2SO_4 solution with and without added inhibitor (10^{-3} M). In uninhibited H_2SO_4 solutions, the EDX spectra (Fig. 11a) confirm the existence of cuprite crystals (Cu_2O), as indicated by the Cu and O signals. However, in inhibited H_2SO_4 solutions (Fig. 11b-h), the EDX spectra showed an additional line characteristic of the existence of C (due to the carbon atoms of SO). In addition, the O signal is significantly enhanced due to the two oxygen atoms present in the carboxylate group of SO. These data show that a carbonaceous material containing oxygen atoms has covered the electrode surface. This layer is undoubtedly due to the inhibitor, because the carbon signal and the high contribution of the oxygen signal are not present on the copper surface exposed to uninhibited H_2SO_4 solutions (see Fig. 11a). In addition, the intensity of the carbon and oxygen signals increase with immersion time (see Figs. 11b-h), since more oleate ions will electrostatically adsorb on the fresh copper surface.

The spectra of Fig. 11b-h show that the Cu peaks are considerably suppressed relative to the

samples prepared in 1.0 M H_2SO_4 solution, and this suppression increases with immersion time. The suppression of the Cu lines occurs because of the overlying inhibitor film. These results confirm those from polarization measurements which suggest that a surface film inhibited the anodic dissolution of copper, and hence retarded the reduction of dissolved oxygen in the H_2SO_4 solution. The inhibitor surface film acts as a barrier to the diffusion of oxygen molecules from solution to copper substrate [42], which may increase the overpotential of cathodic reduction of dissolved oxygen, as shown in Fig. 1. This surface film also increases the polarization resistance of the anodic dissolution of copper (Fig. 6b), slowing down the corrosion rate. This may explain the disappearance of the Warburg impedance at high immersion times and concentrations.

Conclusion:

The polarization and impedance studies of the corrosion inhibition process of copper in 1.0 M H_2SO_4 solution at the corrosion potential using sodium oleate as an anionic surfactant inhibitor showed that the Nyquist diagrams consisted of a capacitive semicircle at high frequencies followed by a Warburg diffusion tail at low frequency values. Addition of SO to H_2SO_4 solution inhibits the corrosion of copper. The inhibition is due to the electrostatic adsorption of the surfactant on the copper surface. EDX observations of the electrode surface showed that a surface film of inhibitor is formed on the electrode surface. This film retarded the reduction of dissolved oxygen and inhibited the growth of copper oxide in the H_2SO_4 solutions (mixed-type inhibitor).

The SO surfactant acts as a mixed-type inhibitor against copper corrosion in H_2SO_4 solutions. The inhibition efficiency increases with the increase of inhibitor concentration but decreases with the increase of temperature. The inhibitor concentration and the immersion time have a great influence on the inhibition efficiency of SO. The inhibition efficiencies obtained from potentiodynamic polarization method are comparable with those obtained from impedance measurements. The data obtained fits well with Temkin adsorption isotherm. The data obtained from two adsorption isotherms are in good agreements.

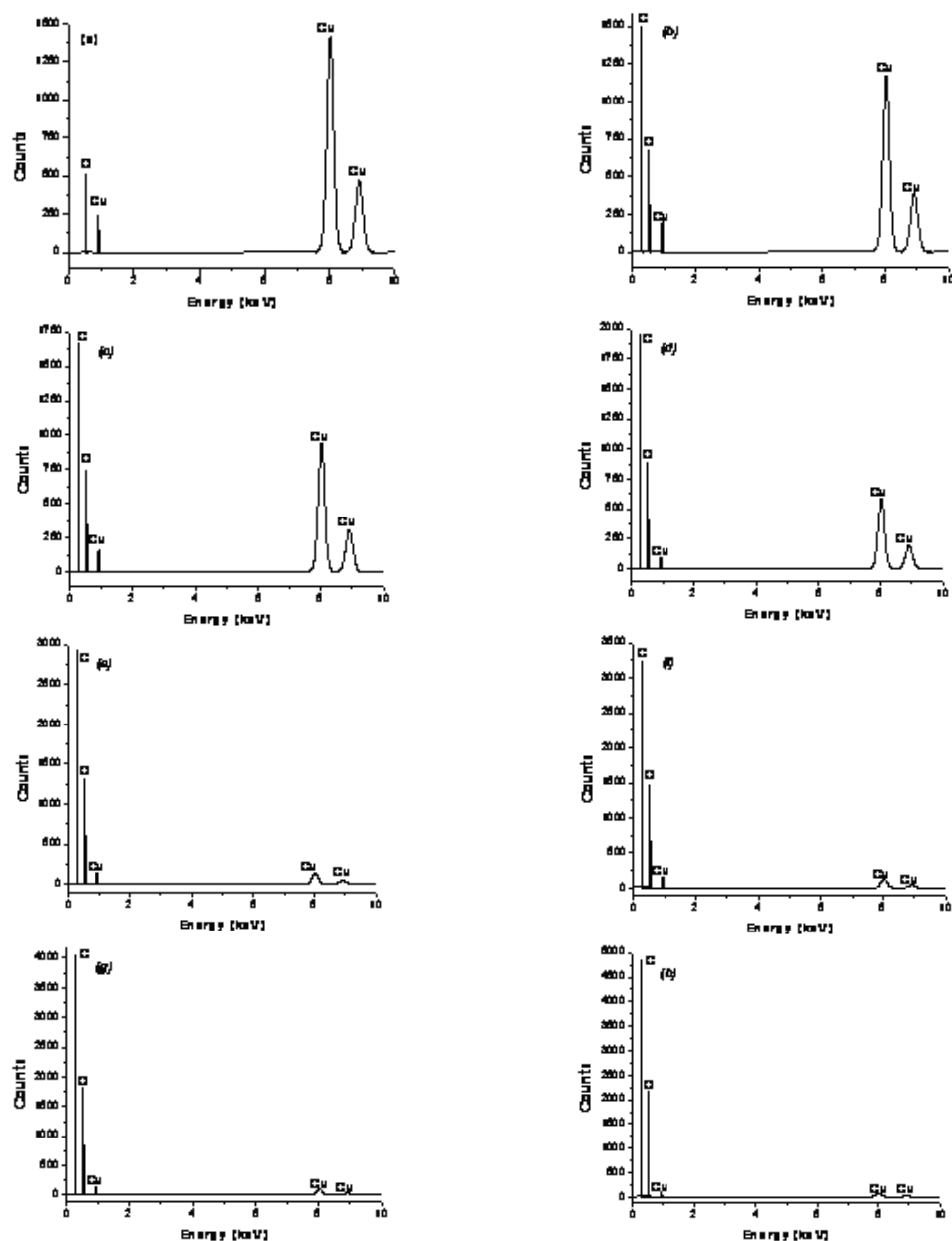


Fig. 11: EDX spectra of copper specimens

- (a) after 30 min of immersion in 1.0 M H_2SO_4 solution.
- (b) after 30 min of immersion in (1.0 M $\text{H}_2\text{SO}_4 + 10^{-3}$ M SO) solution.
- (c) after 60 min of immersion in (1.0 M $\text{H}_2\text{SO}_4 + 10^{-3}$ M SO) solution.
- (d) after 90 min of immersion in (1.0 M $\text{H}_2\text{SO}_4 + 10^{-3}$ M SO) solution.
- (e) after 120 min of immersion in (1.0 M $\text{H}_2\text{SO}_4 + 10^{-3}$ M SO) solution.
- (f) after 150 min of immersion in (1.0 M $\text{H}_2\text{SO}_4 + 10^{-3}$ M SO) solution.
- (g) after 180 min of immersion in (1.0 M $\text{H}_2\text{SO}_4 + 10^{-3}$ M SO) solution.
- (h) after 210 min of immersion in (1.0 M $\text{H}_2\text{SO}_4 + 10^{-3}$ M SO) solution.

Acknowledgements:

The author, Omar A. Hazzazi, wishes to thank Prince Sultan bin Abdulaziz Al-Saud, First Deputy Premier, Minister of Defence and Aviation and Inspector General, and Prince Bandar bin Sultan bin Abdulaziz Al-Saud, the Secretary-General of the National Security Council, for their financial support for this project.

REFERENCES

- [1] S. Aksu and F.M. Doyle, *J. Electrochem. Soc.*, **148**, B51 (2001).
- [2] J. van Muylder, in *Comprehensive Treatise of Electrochemistry*, J. O'M. Bockris, B.E. Conway, E. Yeager, and R.E. White, Editors, Vol. **4**, pp.1, Plenum Press, New York (1981).
- [3] C.A. Sequeira, *Br. Corros. J.*, **30**, 137 (1995).
- [4] M.D. Fallston, in *Corrosion Engineering Handbook*, P.A. Schweitzer, Editor, pp. 89, Marcel Dekker, Inc., New York (1996).
- [5] R. Gasparac, C.R. Martin, E. Stupnisek-Lisac, and Z. Mandic, *J. Electrochem. Soc.*, **147**, 991 (2000).
- [6] D. Tromans and J.C. Silva, *J. Electrochem. Soc.*, **143**, 458 (1996).
- [7] F.M. Al-Kharafi and B.G. Ateya, *J. Electrochem. Soc.*, **149**, B206 (2002).
- [8] H. Ma, S. Chen, S. Zhao, X. Liu, and D. Liu, and D. Li, *J. Electrochem. Soc.*, **148**, B482 (2001).
- [9] G. Trabanelli, in *Corrosion Mechanism*, F. Mansfeld, Editors, pp. 119, Marcel Dekker, Inc., New York (1987).
- [10] H. Luo, Y.C. Guan, and K.N. Han, *Corrosion*, **54**, 619 (1998).
- [11] C.A. Miller, and S. Qutubuddin, in *Interfacial Phenomena in polar Media*, VIII–F, Eike and C.D. Parfitt, Editors, *Surfactant Science Series*, Vol. **21**, pp. 166, Marcel Dekker, Inc., New York (1987).
- [12] S.S. Abd El-Rehim, H.H. Hassan, and M.A. Amin, *Mat. Chem. & Phys.*, **70**, 64 (2001).
- [13] S.S. Abd El-Rehim, H.H. Hassan, and M.A. Amin, *Mat. Chem. & Phys.*, **78**, 337 (2002).
- [14] S.S. Abd El-Rehim, H.H. Hassan, and M.A. Amin, *Corros. Sci.*, **46**, 5 (2004).
- [15] B.A. Boukamp, *Equivalent Circuit*, Princeton Applied Research Corporation, Princeton, N J (1990)}
- [16] E. Mattsson and J. O'M. Bockris, *Trans. Faraday Soc.*, **55**, 1586 (1959).
- [17] W.H. Smyrl, in *Comprehensive Treatise of Electrochemistry*, Vol. **4**, X. O'M. Bockris, B.E. Conway, E. Yeager, and R.E. White, Editors, pp. 116, Plenum Press, New York (1981).
- [18] G.G.O. Cordeiro, O.E. Barcia, and O.R. Mattos, *Electrochim. Acta*, **38**, 319 (1993).
- [19] D.K.Y. Wang, B.A.W. Collier, and D.R. Macfarlane, *Electrochim. Acta*, **38**, 2121 (1993).
- [20] R. Caban and T.W. Chapman, *J. Electrochem. Soc.*, **124**, 1371 (1977).
- [21] O.E. Barcia, O.R. Mattos, N. Pebere, and B. Tribollet, *J. Electrochem. Soc.*, **140**, 2825 (1993).
- [22] H.P. Lee and K. Nobe, *J. Electrochem. Soc.*, **133**, 2035 (1986).
- [23] C. Deslouis and B. Tribollet, *J. Appl. Electrochem*, **16**, 374 (1988).
- [24] F. Bentiss, M. Lagrence, M. Traisnel, J.C. Hornez, *Corros. Sci.*, **41**, 789 (1999).
- [25] G. Moretti, F. Guidi, G. Grion, *Corro. Sci.*, **46**, 387 (2003).
- [26] B.B. Damaskin, O.A. Petrii, B. Batrakov, *Adsorption of Organic Compounds on Electrodes*, Plenum Press, New York, (1971).
- [27] I. Langmuir, *J. Am. Chem. Soc.*, **39**, 1848 (1917).
- [28] R. Alberty and R. Silbey, *Physical Chemistry*, pp. 845, 2nd Edition, Wiley, New York (1997).
- [29] J. O'M. Bockris, S.U.M. Khan, *Surface Electrochemistry: A Molecular Level Approach*, Plenum Press, New York (1993).
- [30] J.W. Schapinik, M. Oudeman, K.W. Leu, J.N. Helle, *Trans. Farad. Soc.*, **56**, 415 (1960).
- [31] A.N. Frumkin, *Z. Phys. Chem.*, **116**, 466 (1925).
- [32] O. Ikeda, H. Jimbo, H. Tamura, *J. Electroanal. Chem.*, **137**, 127 (1982).

- [33] J. Hill de Boer, *The Dynamical Character of Adsorption*, 2nd Edition, Clarendon Press, Oxford, UK, 19683
- [34] H. Dhar, B. Conway, K. Joshi, *Electrochim. Acta*, **18**, 789 (1973).
- [35] E. Kamis, I. Mellucci, R.M. Lantasion, E.S.H. El-Ashry, *Corrosion*, **47**, 677 (1991).
- [36] D. Do, *Adsorption Analysis: Equilibria and Kinetics*, pp. 10-60, Imperial College Press, (1998).
- [37] E. Conway, *Principles of Electrode Processes*, pp. 78-85, The Ronald Press Company, New York (1965).
- [38] S. Martinez, *Mat. Chem. & Phys.*, **77**, 97 (2003).
- [39] W. Durnie, R. De Marco, B. Kinsella, A. Jefferson, *J. Electrochem. Soc.*, **146**, 1751 (1999).
- [40] S. Martinez and I. Stern, *Appl. Surf. Sci.*, **199**, 83 (2002).
- [41] R. Brdicka, O.F. Kemije, S. Knjiga, pp. 460-461, Zagreb (1965).
- [42] M. Ishibashi, M. Itoh, H. Nishihara and K. Aramaki, *Electrochim. Acta*, **41**, 241 (1996).

